# A MEASUREMENT OF THE PROTON WAVEFUNCTION IN MOLECULAR HYDROGEN BY NEUTRON COMPTON SCATTERING

## J Mayers  (Rutherford Appleton Laboratory, Chilton, OX11 0QX)

## Abstract

The momentum distribution of the proton in liquid and solid hydrogen has been measured by neutron Compton scattering (NCS), at energy transfers between 3 and 50 eV. The data display features due to interference between the proton and neutron wavefunctions and are accurately described by a simple quantum mechanical model, incorporating previous spectrocopic data. The excellent agreement between calculation and data in this simple system demonstrates that the NCS technique can provide accurate information about the behaviour of the proton in condensed matter. There are many applications of NCS to more complex physical systems of fundamental interest in physics, chemistry and biology.

# A MEASUREMENT OF THE PROTON WAVEFUNCTION IN MOLECULAR HYDROGEN BY NEUTRON COMPTON SCATTERING

The possibility of measuring nuclear momentum distributions in condensed matter sytems by neutron scattering was first suggested by Hohenberg and Platzmann [1] nearly 30 years ago. The method is analagous to the measurement of electron momentum distributions by Compton scattering [2] and measurement of nucleon momenta by Deep Inelastic Scattering [3] and is known as Neutron Compton Scattering (NCS) or Deep Inelastic Neutron Scattering (DINS). The theoretical basis of all three techniques is the impulse approximation (IA), which is exact when the momentum transfer $\vec{q}$ and energy transfer $\omega$ are infinite [4,5,6]. When the IA is valid, the scattering cross section is proportional to the distribution of nuclear momentum components along the direction of $\vec{q}$ and can be used to determine $n(\vec{p})$, the distribution of nuclei (and hence atoms) in momentum space.

NCS measurements on protons have a particularly simple interpretation, as the interaction of protons with other atoms can usually be accurately accounted for [7,8] in terms of a single particle potential and hence by a proton wavefunction. From elementary quantum mechanics, $n(\vec{p})$ is related to the Fourier transform of the proton wavefunction $\Psi(\vec{r})$ via,

$$n(\vec{p}) = \frac{1}{(2\pi)^3} \left| \int \Psi(\vec{r}) \exp(i\vec{p}.\vec{r}) d\vec{r} \right|^2 \tag{1}$$

and an NCS measurement of $n(\vec{p})$ can be used to determine the wavefunction in an analagous way to the determination of real space structure from a diffraction pattern. In principle such measurements can provide very detailed information about the behaviour of the proton in a variety of systems of fundamental interest in physics, chemistry and biology.

NCS measurements on protons have only become possible since the construction of intense accelerator based neutron sources , which have allowed accurate inelastic neutron scattering measurements with energy transfers in the eV region [9]. For NCS measurements on the proton in molecular hydrogen, energy transfers much greater than the vibrational frequency of the molecule (516 meV [10]), are required before the IA can be used to reliably determine $n(\vec{p})$. At lower energy transfers the IA is no longer valid and $n(\vec{p})$ is not related

in a simple way to the observed scattering intensities. In sytems with weaker binding, lower energy transfers can be used and many early NCS measurements were performed on helium at relatively low energy and momentum transfers, ($\omega$ < 300 meV and $q$ < 15 Å$^{-1}$). These studies were motivated primarily by the possibility of directly observing the Bose condensate fraction in superfluid $^4$He [11,12,13,14,15]. More recently NCS measurements with 15<$q$<40 Å$^{-1}$ and incident energies up to 2 eV have been made on condensed phases of helium[16] and neon[17]. There have been a few pioneering studies on various systems at eV energy transfers [18,19,20]. Measurements on molecular hydrogen have also been made, with $\omega$ insufficient to excite vibrational transitions [21,22]. This allows a measurement of the centre of mass motion of $H_2$ molecules rather than the momentum distribution of individual protons. The measurements described here were made with 3<$\omega$<50 eV and 30<$q$<130Å$^{-1}$. At such high values of $q$ and $\omega$, accurate NCS measurements can be made even in strongly bound systems such as hydrogen.

The formal statement of the IA in neutron scattering is [23]

$$S(\vec{q},\omega) = \int n(\vec{p})\delta\left(\omega + \frac{p^2}{2M} - \frac{(\vec{p}+\vec{q})^2}{2M}\right)d\vec{p}$$ (2)

where $S(\vec{q},\omega)$ is the dynamic structure factor, $n(\vec{p})$ is the nuclear momentum distribution, $\vec{p}$ is the atomic momentum and $M$ is the nuclear mass. The $\delta$ function expresses the conservation of kinetic energy, which applies to the collision between the nucleus and the neutron when the IA is satisfied. When the scattering sample is isotropic it can be shown that [5],

$$S(q,\omega) = \frac{M}{q}J(y)$$ (3)

where

$$y = \frac{M}{q}\left(\omega - \frac{q^2}{2M}\right)$$ (4)

and

$$J(y) = 2\pi\int_{|y|}^{\infty} pn(p)dp$$ (5)

$J(y)dy$ is the probability that an atom has momentum component along $\vec{q}$ with magnitude between $y$ and $y+dy$ and is known as the Compton profile. Equations 3 to 5 express the `$y$ scaling' property of the neutron cross section at sufficiently high $q$ [24].

The measurements were performed on the electron volt spectrometer eVS at the ISIS neutron source [25]. A filter difference technique [26], with a gold foil anlayser, was used to fix the energy of the scattered neutron at 4.922 eV. Time of flight techniques [27] were used to determine the energy of the scattered neutron and hence $S(q,\omega)$. The sample of para hydrogen was measured at temperatures of 20K and 4K (the liquid and solid phases respectively) and was a 5% scatterer, contained in a planar aluminium can with a sample thickness of ~1mm and with the sample plane perpendicular to the incident beam. Measurement times were 24 hours at each temperature. Due to the $y$ scaling property mentioned above, all scans through $q,\omega$ space map on to the same function $J(y)$. Thus providing the IA is well satisfied the measurements of $J(y)$ at different angles differ only in the width of the instrument resolution function and can be averaged to improve statistical accuracy. As the differences observed between the 4.9K and 20K data were at the limits of measurement accuracy, the data sets at the two temperatures were also averaged to further reduce the statistical error.

Figure 1a shows the average of Compton profiles measured in 10 $^3$He gas detectors at angles between 35 and 45°, Figure 1b that for 10 detectors between 45 and 55° and 1c for 20 detectors at angles between 55 and 75°. The instrument resolution function [25,28] is also shown for each of these data sets, together with the energy and momentum transfers corresponding to the detector at the centre of each bank. There is a small multiple scattering component in the data which is visible at large positive $y$ values, particularly in the data sets at the two lower angles and this has been fitted by a second order polynomial. The data shows small systematic shifts of the peak of the distribution towards negative $y$, due to inaccuracies in the IA which are present at the finite $q$ of the measurement. It has been shown by Sears [5] that symmetrisation of data about $y = 0$ removes most of these inaccuracies and this procedure has been followed to produce the data shown in Figure 2. The data from all detectors between

35° and 55° has been averaged and the multiple scattering background subtracted before symmetrisation.

The results are well described by a simple quantum mechanical model. It is assumed that the hydrogen molecule is bound by a harmonic potential and that its centre of mass translational motion is independent of its vibration along the bond axis. $J(y)$ is then the convolution of the momentum distributions for the vibrational and translational motions considered separately.

$$J(y) = \int J_T(y')J_V(y' - y)dy' \tag{6}$$

The translational momentum distribution $J_T(y)$ is approximated by a Gaussian function.

$$J_T(y) = \frac{1}{\sqrt{2\pi\sigma_T^2}}\exp\left(\frac{-y^2}{2\sigma_T^2}\right) \tag{7}$$

From previous measurements [21] the kinetic energy of the centre of mass motion is 63 ±6K in the liquid at 17K and 76±9 in the solid at 10K. Taking the average of these values as 70K, the translational kinetic energy of each atom is 35K $=3\sigma_T^2/(2M)$ and $\sigma_T=0.70$ Å$^{-1}$.

The momentum distribution $J_V(y)$ associated with vibration along the bond can be determined from the wave function of the proton in the molecule. Since the binding is assumed harmonic, each atom will have a Gaussian probability distribution along the bond axis, centred at its mean position at distance $R$ from the centre of mass, where $2R$ is the bond length. In parahydrogen below 20K only the J=0 state of rotation is thermally occupied and the molecular wavefunction has no directional dependence. Thus the wave function of each proton is a spherical shell.

$$\Psi(r) = \left[2\pi^{3/2}\sigma(\sigma^2 + 2R^2)\right]^{-1/2}\exp\left[\frac{-(r-R)^2}{2\sigma^2}\right] \tag{8}$$

where the mean square displacement of the atom from its mean position along the bond is $\sigma^2/2$ $(=\int r^2|\Psi(\vec{r})|^2 dr)$. Neglecting terms of order $erfc[R^2/(2\sigma^2)]$ equations 1 and 8 give,

$$n(p) = \frac{2\sigma}{\pi^{3/2}p^2(\sigma^2 + 2R^2)}\left(p\sigma^2\cos pR + R\sin pR\right)^2\exp\left(-\sigma^2 p^2\right) \qquad (9)$$

The bond length is accurately known from spectroscopic measurements ($R$=0.3405 Å [10]) and the value of $\sigma$ can be determined from the frequency of molecular vibration as $\sigma = 0.1269$ Å . The solid line in Figures 1a-1c is fit to a convolution of the model $J(y)$ with the resolution function. The only fitting parameters are a scale factor, the position of the distribution and the polynomial coefficients, which account for the multiple scattering background. The values of $\sigma$ ,$R$ and $\sigma_r$ were fixed at the values given above. It can be seen that the model gives excellent agreement with the measurements at all angles. The solid line in Figure 2a is the calculated $J(y)$ after convolution with the resolution function- there are no free parameters. The difference between the predictions of the model and the symmetrised data is shown in figure 2b as the points oo. A fit to the data shown in figure 2a, with $R$ and $\sigma$ as free parameters gave $R$=0.356± 0.003 Å and $\sigma$=5.70±0.03 Å$^{-1}$, in good agreement with the values of 0.37 and 5.577 obtained from spectroscopy, although outside the quoted statistical error, due to small systematic errors.

The importance of including the oscillatory terms in equation 9 is demonstrated by the predictions of a classical model, which neglects the wave nature of the proton. It is assumed that the molecule is a classical linear vibrator and that each proton has a Gaussian momentum distribution along the bond. Averaging over all possible directions of the bond axis in space, to take account of the isotropy of the sample gives

$$n(p) = \frac{1}{2\pi p^2}n_V(p) \qquad (10)$$

where $n_V(p)$ is the distribution of momentum components along the bond. A calculation using equations 5,6,7 and 10 gives the results shown as the dashed line in Figure 2a. The difference between the classical and the quantum models is shown as the solid line in figure 2b and displays oscillations with a first maximum at $y \approx \pi/(2R)$. This is well reproduced by the data points xx, which are the difference between the data and the classical prediction. The oscillations in

the data are the first observation of interference between the proton and neutron wavefunctions.

The future applications of NCS measurements from protons and deuterons are very wide. An example is the hydrogen bond where NCS can determine whether the observed bi-modal distribution of the proton in hydrogen bonds is the result of statistical or quantum disorder [29]. The information obtained from NCS is qualitatively different to that given by neutron diffraction measurements. The latter determine an infinite time average of the spatial distribution of the proton wheras the former measures the proton wavefunction on a very short timescale. Thus NCS can distinguish between quantum tunneling and thermally induced hopping of the proton between different sites. One application is to the study of the mechanism of protonic diffusion in metals, semiconductors and ionic conductors. Another is to the determination of the proton wavefunction in molecules which undergo rotational tunnelling [30].

The very close agreement between data and calculation in this simplest of protonic condensed matter systems, demonstrates that NCS measurements have now reached a high level of accuracy. It shows that wavefunctions of protons can be determined even in isotropic samples, such as liquids, powders, amorphous materials and polymers. Much more detailed information about the proton wavefunction can be obtained from single crystal samples, where NCS allows a model independent reconstruction of both the proton wavefunction and the potential well of the proton in three dimensions [29]. Orders of magnitude increases in the accuracy of NCS measurements will soon be produced by improvements in countrate and resolution and it seems certain that future measurements will provide precise and unique information about the short time dynamics of protons, in many condensed matter systems of fundamental physical interest.

## References

1 P. C. Hohenberg and P. M. Platzmann, Phys Rev **152**, 198 (1966)

2 P. M. Platzmann in `Momentum Distributions', ed R. N. Silver and P. E. Sokol (Plenum Press,New York, 1989, p249)

3 I Sick in ref 2, page 175.

4 R Newton, 'Scattering Theory of Waves and Particles', (Springer, Berlin, 1981)

5 V. F. Sears Phys. Rev. B **30**, 44 (1984)

6 J. Mayers Phys. Rev. B **41**,41 (1991)

7 R. Hempelmann, D. Richter and D. L. Price Phys. Rev. Lett. **58**, 1016 (1987)

8 M. Warner, S. W. Lovesey and J. Smith Z. Phys. B **39**, 2022 (1989)

9 R. S. Holt, J. Mayers and A. D. Taylor in ref 2 , p. 295

10 I. F. Silvera, Rev. Mod. Phys. **52**, 393 (1980)

11 R. A. Cowley and A.D. B. Woods, Phys. Rev. Lett. **21**, 787 (1968)

12 O. K. Harling, Phys. Rev. Lett. **24**, 1046 (1970)

13 H. A. Mook, Phys. Rev. Lett. **32**, 1167 (1974)

14 H. A. Mook, Phys. Rev. Lett. **51**, 1454 (1983)

15 P. Martel, E. C. Svensson, A. D. B. Woods, V. F. Sears and R. A. Cowley, J. Low Temp. Phys. **23**, 285 (1976)

16 T. R. Sosnick, W. M. Snow, and P. E. Sokol, Phys. Rev. B **41**, 11185 (1990)

17 D. A. Peek, M. C. Schmidt, I. Fujita and R. O. Simmons, Phys. Rev. B **45**, 9671 (1992) and **45**, 9680 (1992)

18 H. Rauh and N. Watanabe, Phys. Lett. **100A**, 244 (1984)

19 M. P. Paoli and R. S. Holt, J. Phys. C **21**, 3633 (1988)

20 S. Ikeda, K. Shibata, Y. Nakai amd P. W. Stephens, J. Phys. Soc. Japan **61**, 2619 (1992)

21 W. Langel, D. L. Price, R. O. Simmons and P. E. Sokol, Phys Rev B 38,11275 (1988)

22 K. W. Herwig, J. L. Gavilano, M. C. Schmidt and R. O. Simmons, Phys. Rev. B **41**, 96 (1990)

23 S. W. Lovesey, ` Theory of Neutron Scattering from Condensed Matter', (Oxford University Press, New York,1987)

24 G. B. West in ref 2, p95.

25 J. Mayers and A. C. Evans, Rutherford Laboratory Report, RAL-91-048 (1991)

26 P. A. Seeger, A. D. Taylor and R. M. Brugger, Nuc. Inst. Meth, **A240**, 98 (1985)

27 C. G. Windsor, `Pulsed Neutron Scattering', (Taylor and Francis, London, 1981)

28 C. Andreani, G. Baciocco, R. S. Holt and J. Mayers Nuc. Inst. Meth. **A276** , 297 (1989)

29 G. Reiter and R. N. Silver, Phys. Rev. Lett. **54**, 1047 (1985)

30 W. Press, `Single Particle Rotations in Molecular Crystals' (Springer, Berlin, 1981)

## Figure Captions

### Figure 1.

The data points are the average of the measured neutron Compton profiles obtained from detectors in three different angular ranges. (a) $35°-45°$, (b) $45°-55°$, (c) $55°-75°$. The solid line is the fit described in the text. The resolution function is shown for each data set as a dashed line.

### Figure 2

In (a) the points oo are the sum of data from 20 detectors at scattering angles between $35°$ and $55°$ after subtraction of multiple scattering and symmetrisation. The solid line is the calculation using equation 9 and the dashed line that using equation 10, both after convolution with the instrument resolution function. Figure 2b shows the difference between the data and the two models. oo equation 9, xx equation 10. The solid line is the difference between the quantum and classical models.
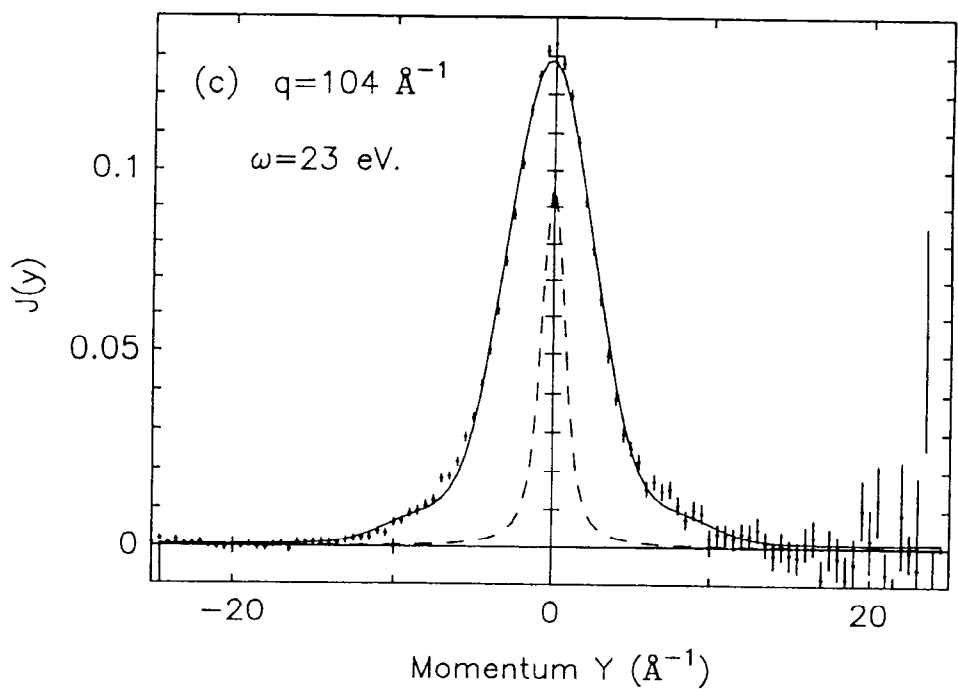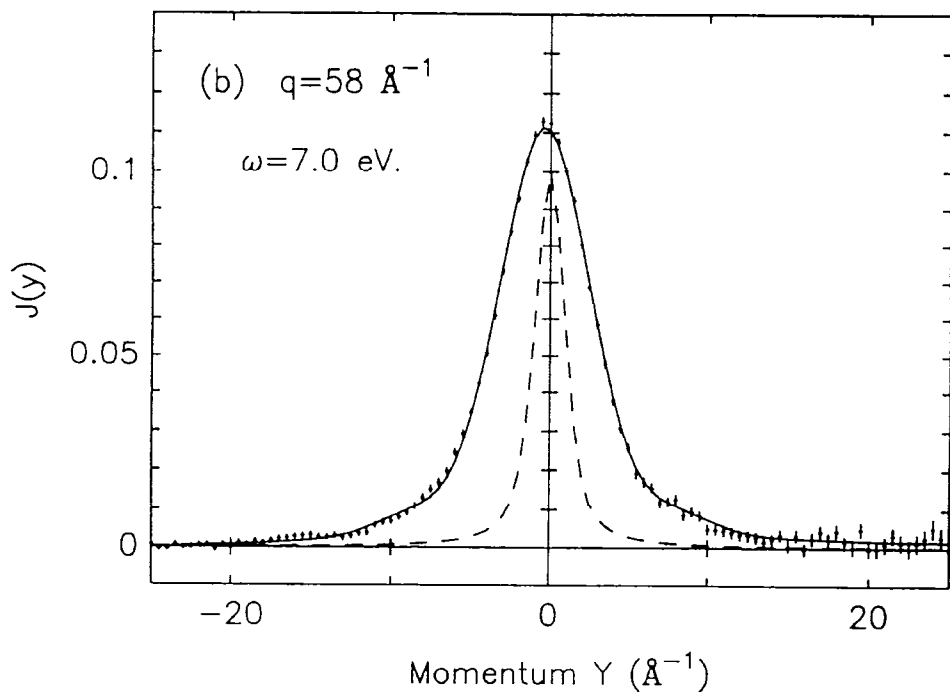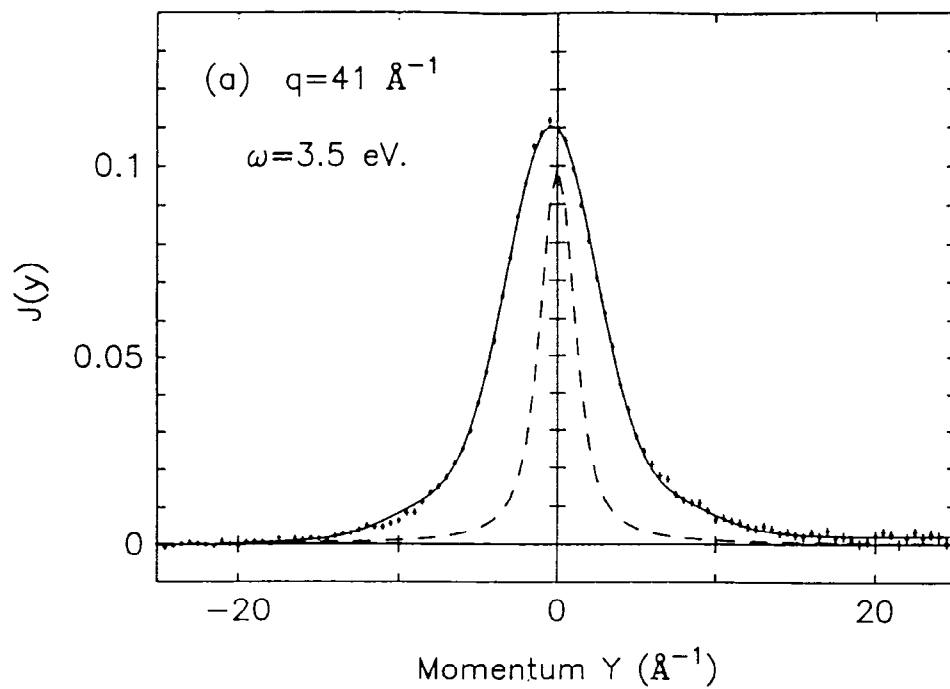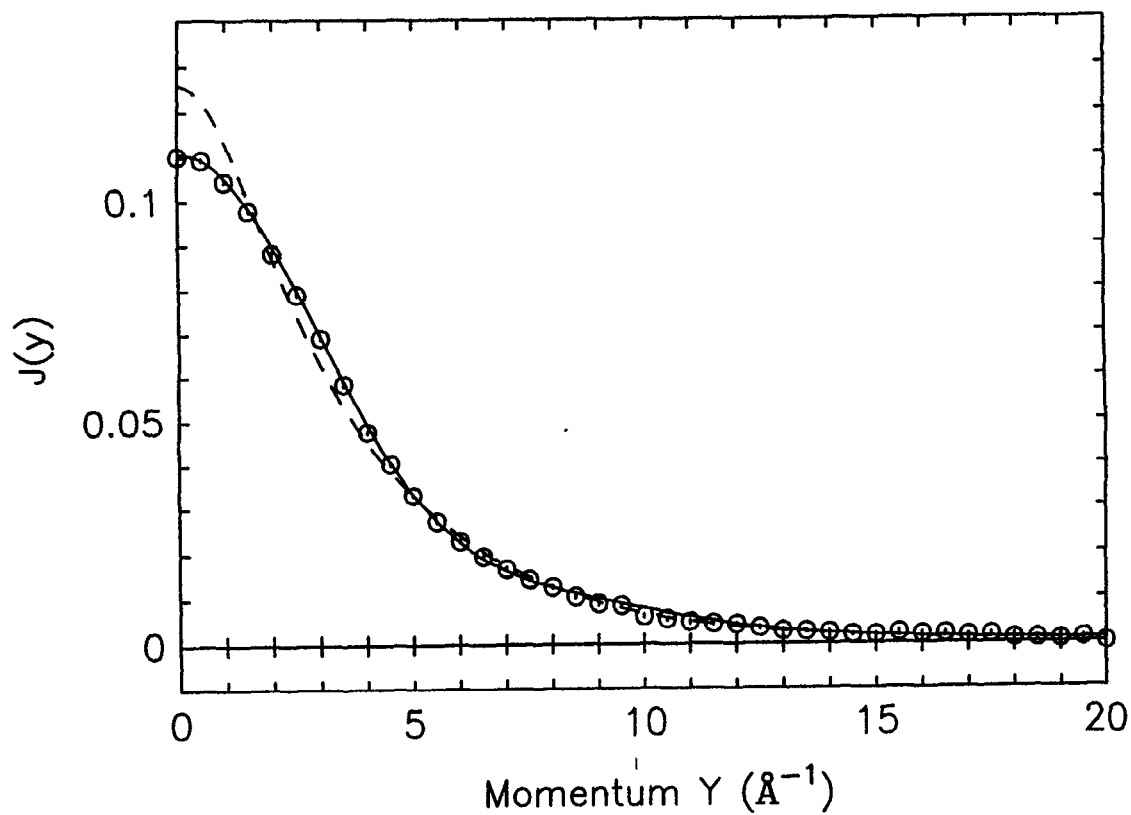
Fig. 1.

(a) q=41 Å$^{-1}$

ω=3.5 eV.

(b) q=58 Å$^{-1}$

ω=7.0 eV.

(c) q=104 Å$^{-1}$

ω=23 eV.

## Figure 2a.



## Figure 2b